DOI: 10.48368/bgs-2025.1.n2

Pi2 pulsations during the main phase of the geomagnetic storm on May 10-11, 2024.

Maria Chamati[1]

[1]National Institute of Geophysics, Geodesy and Geography, Bulgarian Academy of Sciences,
mail: mchamati@geophys.bas.bg

Key words: extreme, geomagnetic, Panagjurishte, Pi2, storm, ULF

Summary
In this study, the spectral characteristics of irregular ULF (ultra-low frequency) geomagnetic pulsations – Pi2 with periods of 40-150 s (6.7-25 mHz) during the main phase of the extreme geomagnetic storm on May 10-11, 2024 – are presented. Data records with resolution 1s of the magnetometer located at the Geomagnetic Observatory Panagjurishte are analysed. By using a band-pass filtering procedure, based on the fast Fourier transform, fifteen frequency ranges within the definition of this type of pulsation have been obtained. It was found that Pi2 pulsations accompany the main phase of the storm and, at mid-latitudes at the point of recording, it is most intensive in the frequency range 8-20 mHz during 18-02 UT (21-05 MLT).

Introduction

On May 10-13, 2024, an extreme geomagnetic storm (Kp=9, local K index=9 (Metodiev, M. and Trifonova, P., 2021)) took place on Earth (Hayakawa et al., 2025). During this storm, due to appropriate conditions of solar wind (SW) parameters, such as high values of dynamic pressure that persist for a relatively long time, several super-substorms were generated.
Pi2 irregular geomagnetic pulsations with periods in range 40-150s are ultra-low frequency waves (ULF), that are important for understanding the physical processes driving the onset of substorms. The high-speed plasma flows in Earth's magnetosphere, triggered during the substorm, generated compressional waves (Takahashi et al., 2018). These waves then couple to the plasmasphere, exciting resonances that reach the ionosphere. There, they drive ionospheric currents, which excite pulsations that are observed in the variations of Earth's magnetic field. Its spatial and temporal characteristics provide useful information about the processes occurring in the magnetosphere and ionosphere during substorms (McPherron, 2023; Mishin et al., 2020; Rae et al., 2017).
They can be observed even at very low geomagnetic activity (Ghamry, 2017).

Data and methods

The data sets with resolution 1s recorded by three-axial induction magnetometer installed in the Geomagnetic Observatory Panagjurishte, Bulgaria, were used. The three axes are oriented along north-south, east-west and down directions. They correspond to the geomagnetic vector components X, Y and Z.
For the purpose of our findings, the fast Fourier transform and band-pass filtering procedure were used to extract Pi2 pulsations in different frequency bands.

Results

Figure 1 depicts solar wind (SW) parameters – the flow pressure and the flow speed; the south component (Bz) of the interplanetary magnetic field (IMF); Kp and Dst indices that represent the degree of perturbation of the geomagnetic field and the onset of the storm, respectively. The Dst index points to the main phase of the storm at about 18 UT on May 10 and its end about 00-01 on May 11 (marked in the dashed rectangle on the figure), when it reaches its minimal value -406 nT. The flow speed and pressure rise simultaneously during the main phase of the storm. The flow speed reaches a value of about 700 km/s, and the flow pressure reaches 51 nPa. The Bz component of IMF decreased to -47 nT. Kp index had values 8-9. The geomagnetic variations along X and Y components, recorded in the Geomagnetic Observatory Panagjurishte during the main phase of the storm, are depicted in Figure 2. The X component is red, and Y component is in green color.

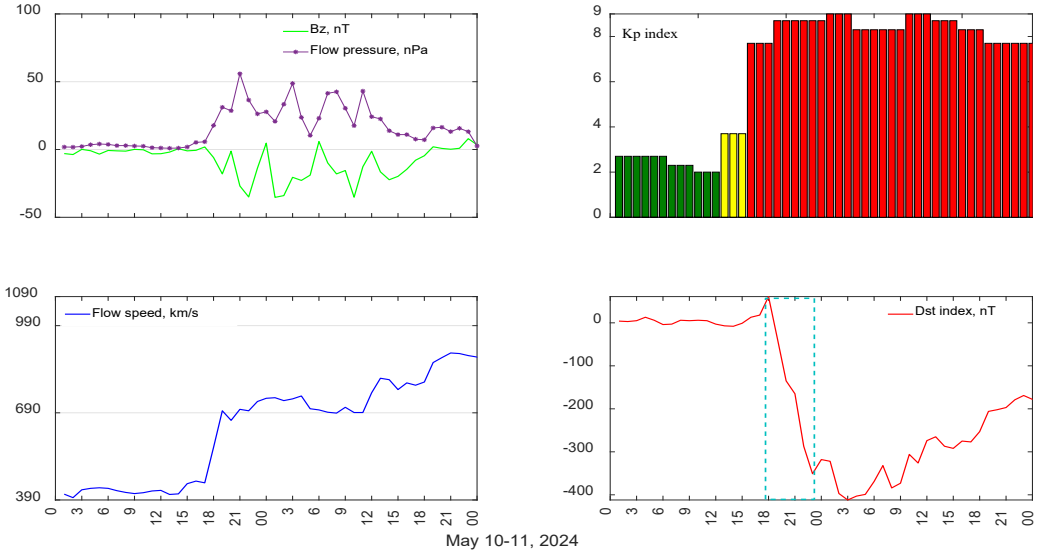


Figure 1. Solar wind parameters and geomagnetic conditions

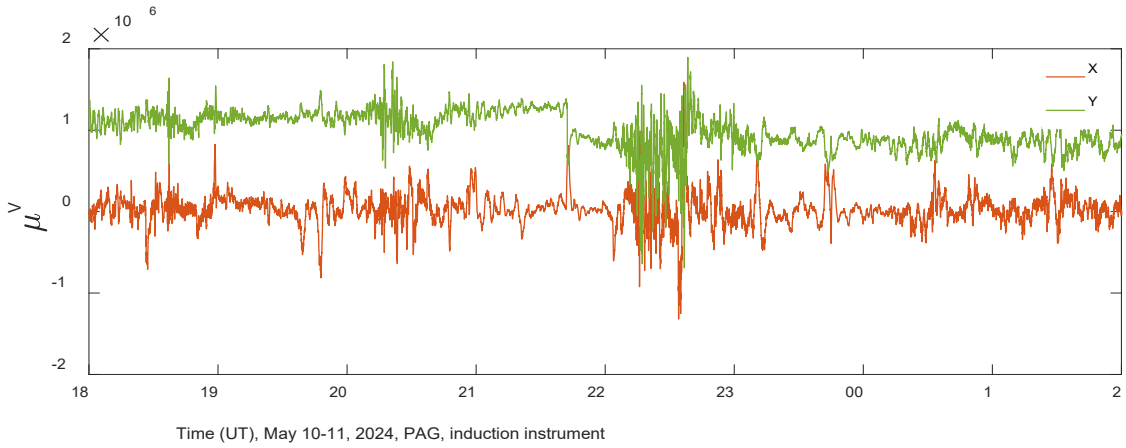


Figure 2. Geomagnetic variations along X and Y components

The bandpass filtering procedure is applied to the data set from X component values of recordings and Pi2 pulsations according to Jacobs classification (Jacobs et al., 1964) are extracted (Figure 3).

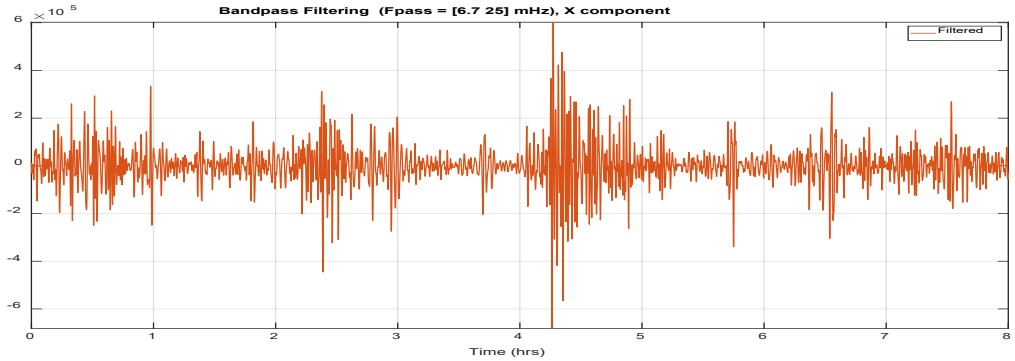


Figure 3. Bandpass filter 6.7-25*mHz*, X component, 18-02UT, May 10-11

The band-pass filter contains all frequencies according to the official classification as mentioned above. Here, a few "packets" of ULF irregular waves are observed during the time interval 18-02 on May 10-11. The time interval covers

the main phase and two hours after the main phase of the storm. A total of 15 frequency sub-bands (not presented) of the main classification of these waves were examined in more detail. On Figure 4 the frequency range 8-20 *mHz* is presented in eight squares (hour by hour), as more clearly and powerful manifestation of Pi2. In the time interval 22-23UT the amplitudes of these pulsations are the largest along the X component. Its maximal value reaches $5.5x10^5$ μV.

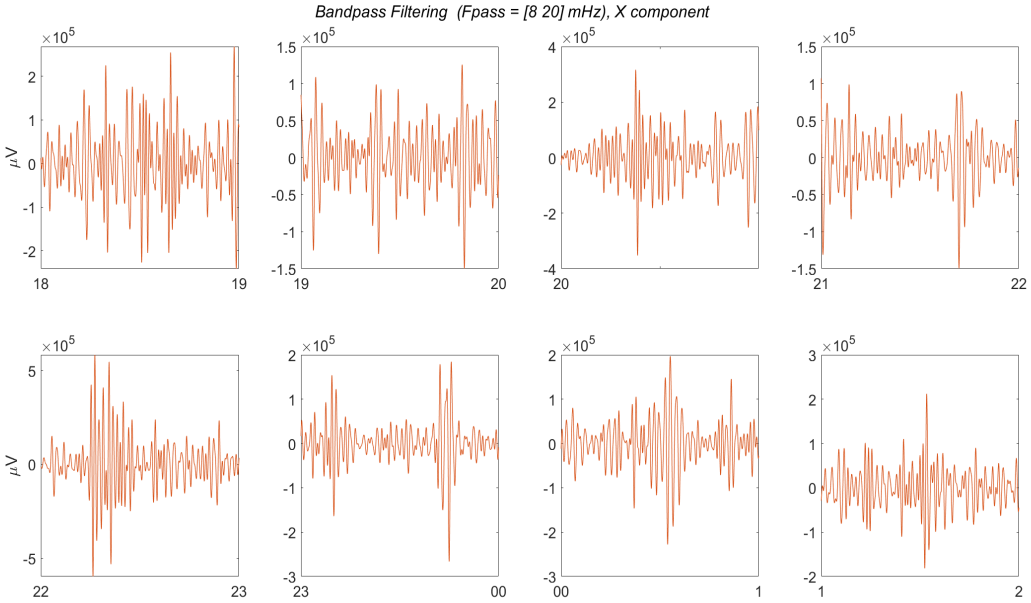


Figure 4. Bandpass filter 8-20*mHz*, X component

The same procedure is applied for the Y component. Figure 5 depicts the full band of frequencies of Pi2 according to the official classification. Compared with Figure 3, the time interval 22-23UT contains amplitudes larger than those along the X component. It may depend on the angle penetration of the disturbance and the change of solar wind speed, and its dynamic pressure as shown on Figure 1.

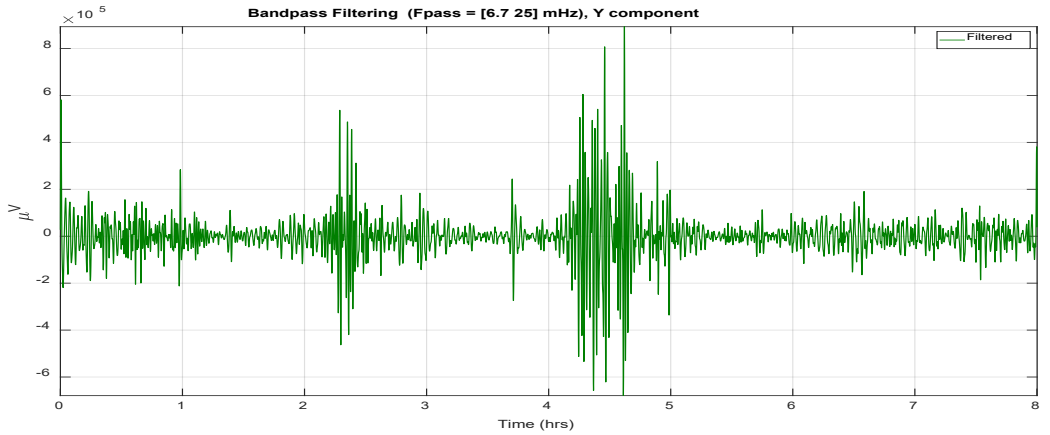


Figure 5. Bandpass filter 6.7-25*mHz*, Y component, 18-02UT, May 10-11

After that, the most intensive Pi2 pulsations are extracted along the Y component in the frequency band *8-20 mHz* during the time interval 22-23 UT (Figure 6). Comparing Figures 4 and 6, the Pi2 pulsation differs in shape and amplitude along X and Y directions.

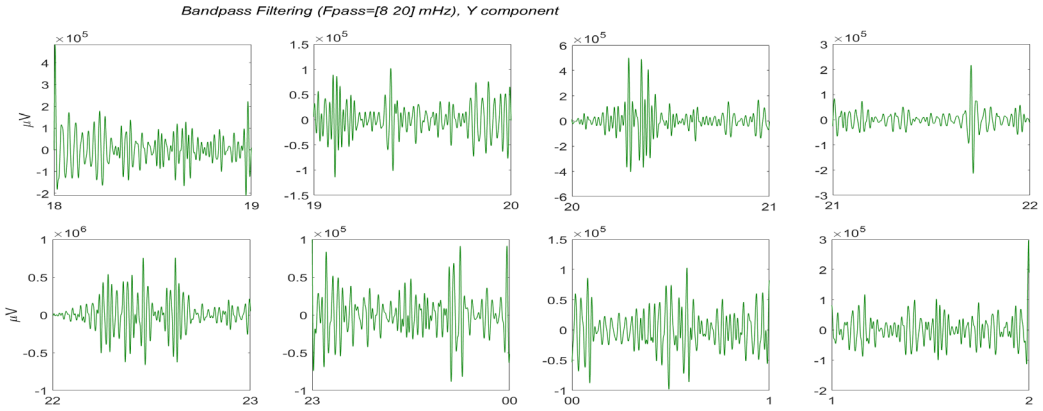


Figure 6. Bandpass filter 8-20*mHz*, Y component

Conclusions

The ULF geomagnetic irregular pulsations (Pi2) during the main phase (18-02UT) of the extreme geomagnetic storm on May 10-11, 2024, are studied. Applying band-pass filtering procedure based on fast Fourier transform (FFT) over the fifteen different frequency bands along the X and Y components, the most intensive manifestation of Pi2 was found in band-pass 8-20 mHz during the main phase of the storm when Kp=9. It has also been found that Pi2 pulsations differ in shape and amplitude depending on the direction of propagation of the ULF waves.

Funding. This study is supported by Contract No D01-321/30.11.2023 (Project "National Geoinformation Center (NGIC))", financed by the National Roadmap for Scientific Infrastructure 2020-2027 of Bulgaria.

Acknowledgements. We thank the OMNIWEB database (https://omniweb.gsfc.nasa.gov/form/dx1.html) for the data provided (Kp, Dst, Bz, SW speed, flow pressure) and the real-time data provided by Geomagnetic Observatory Panagjurishte, Bulgaria (https://pagmag.ngic.bg/).

References

Ghamry E (2017) Pi2 pulsations during extremely quiet geomagnetic condition: Van Allen Probe observations. J. Astron. Space Sci. 34: 111–118. https://doi.org/10.5140/JASS.2017.34.2.111

Hayakawa H, Ebihara Y, Mishev A, Koldobskiy S, Kusano K, Bechet S, Yashiro S, Iwai K, Shinbori A, Mursula K, Miyake F, Shiota D, Silveira MVD, Stuart R, Oliveira DM, Akiyama S, Ohnishi K, Ledvina V, Miyoshi Y (2025) The solar and geomagnetic storms in 2024 May: A flash data report. Astrophys. J. 979: 49. https://doi.org/10.3847/1538-4357/ad9335

Jacobs JA, Kato Y, Matsushita S, Troitskaya VA (1964) Classification of geomagnetic micropulsations. J. Geophys. Res. 69: 180–181. https://doi.org/10.1029/JZ069i001p00180

McPherron RL (2023) Substorm triggering by the solar wind. J. Geophys. Res. Space Phys. 128: e2022JA031147. https://doi.org/10.1029/2022JA031147

Metodiev M, Trifonova P (2021) Local geomagnetic K-indices calculated at PAG observatory since 2007. National Institute of Geophysics, Geodesy and Geography, Bulgarian Academy of Sciences. https://doi.org/10.34975/ctlg-2021.k-ind.v.1

Mishin VV, Tsegmed B, Klibanova YuYu, Kurikalova MA (2020) Burst geomagnetic pulsations as indicators of substorm expansion onsets during storms. J. Geophys. Res. Space Phys. 125: e2020JA028521. https://doi.org/10.1029/2020JA028521

Rae IJ, Murphy KR, Watt CEJ, Mann IR, Yao Z, Kalmoni NME, Forsyth C, Milling DK (2017) Using ultra-low frequency waves and their characteristics to diagnose key physics of substorm onset. Geosci. Lett. 4: 23. https://doi.org/10.1186/s40562-017-0089-0

Takahashi K, Hartinger MD, Vellante M, Heilig B, Lysak RL, Lee D-H, Smith CW (2018) Roles of flow braking, plasmaspheric virtual resonances, and ionospheric currents in producing ground Pi2 pulsations. J. Geophys. Res. Space Phys. 123: 9187–9203. https://doi.org/10.1029/2018JA025664